https://doi.org/10.5194/egusphere-2025-2466
Preprint. Discussion started: 24 June 2025

The impact of tropical cyclones on regional ozone pollution and its future trend in the Yangtze River Delta of China

Mengzhu Xi[1], Min Xie[1, 2*], Yi Luo[3], Danyang Ma[1], Lingyun Feng[1], Shitong Chen[1], Shuxian Zhang[1]

[1] School of Environment, Nanjing Normal University, Nanjing 210023, China

[2] Carbon monitoring and digital application technology center, Carbon peak and carbon neutralization strategy institute of Jiangsu Province, Nanjing 210023, China

[3] Ningbo Ecological Environment Monitoring Center of Zhejiang Province, Ningbo 315048, China

Correspondence to: Min Xie (minxie@njnu.edu.cn)

Abstract: Tropical cyclones (TCs) have a significant impact on ozone (O_3) in coastal regions by affecting atmospheric circulation and meteorological conditions. This paper investigates the impact and its future changing trends in the Yangtze River Delta (YRD) region. It was found that regional O_3 pollution usually occurred before TCs made landfall and after they dissipated in 2018-2022. Using rotation principal component analysis in T-mode (PTT) method, five main synoptic weather patterns (SWPs) are identified. The TC weather pattern (SWP5) is a high-frequency weather pattern in summer (72.22%). Subsequently, with the aid of the data reconstruction of O_3 concentrations, how SWPs, especially TCs, affect O_3 is quantified. It is found that the intensity of SWPs is the dominant factor for the annual variation sequence of O_3, contributing 81.39% to the change in O_3 annual concentrations. Finally, based on future climate scenario data, the changes in TCs and their impact on the trend of O_3 are discussed. Under the SSP2-4.5 scenario, the O_3 in the warm seasons of the YRD is expected to increase by 8.3 μg/m^3 compared with the historical period, and the SWP5 is expected to contribute the most to the estimated O_3 concentration in 2030 (15.14%). Under the SSP5-8.5 scenario, the O_3 will increase by 10.9 μg/m^3. The SWP5 is expected to contribute the most to the estimated O_3 in 2060 (20.66%). This shows that the intensification of climate change will intensify the impact of TCs on O_3 in the YRD, and monitoring and early warning need to be strengthened.

1 Introduction

In recent years, the concentration of ground-level O_3 in many cities in China has significantly exceeded standards and has intensified. O_3 has replaced Particulate Matter (PM) as the primary pollutant in many regions (Wang et al., 2023; Yang et al., 2025; Zhao et al., 2020). Ground-level O_3 is mainly generated by photochemical reactions of volatile organic compounds (VOCs) and nitrogen oxides (NO_x) under sunlight (Zhang et al., 2024; Lu et al., 2019). High concentrations of O_3 can damage the human respiratory system, destroy the human immune system, and even increase the risk of death (Gong et al., 2024; Wang et al., 2025). It can also damage the ecosystem, causing plant leaf necrosis and crop yield reduction (Li et al., 2024). In the past years of YRD, high emissions of motor vehicle and industrial waste gases, coupled with complex terrain and meteorological conditions due to urbanization, have led to complex air pollution characterized by high O_3 and PM concentrations (Zhan et al., 2024). According to the 2020 China Ecological Environment Bulletin, in many Chinese cities, the number of days with air quality exceeding the standard with O_3 as the primary pollutant accounted for over 50% of the total

https://doi.org/10.5194/egusphere-2025-2466
Preprint. Discussion started: 24 June 2025

number of days exceeding the standard.

O_3 concentration is regulated by precursor emissions and meteorological conditions during its generation process (Xie et al., 2016; Gong et al., 2022; Xu et al., 2023b). Meteorological factors such as temperature, humidity, precipitation, atmospheric stability, and mixing layer height play important roles in the emission, transportation and dispersion, chemical reaction, and dry and wet deposition of air pollutants (Chen et al., 2020; Li et al., 2020). Regional O_3 pollution events are often triggered by meteorological conditions such as strong radiation, high temperature, low relative humidity, and low wind speed (Zhan and Xie, 2022; Wang et al., 2024b). Changes in meteorological conditions are affected by weather systems, and the role of weather systems in O_3 concentrations changes has also received widespread attention.

TC activities have a profound impact on the ecological environment of China's coastal areas. In the summer and autumn seasons when O_3 pollution is frequent, TCs are one of the key weather systems that induce O_3 pollution in the YRD (Shu et al., 2016; Zhan and Xie, 2022; Qi et al., 2024). Although the strong winds and precipitation brought by landfalling TCs have a strong scavenging effect on pollutants, the peripheral circulation of TCs away from lands will significantly change the temperature field, wind field, and boundary layer structure, thereby affecting the chemical and physical processes related to O_3 generation, transport, dispersion and deposition, which may in turn aggravate O_3 pollution (Lam et al., 2005; Yang et al., 2012; Jiang et al., 2015; Chow et al., 2018; Xu et al., 2023a). Deng et al. (2019) found that under the influence of the peripheral circulation of TCs, the Pearl River Delta (PRD) is prone to high temperature, low humidity, low wind speed, and strong radiation, which leads to the occurrence of high O_3 and PM concentrations. Hu et al. (2023) focused on analyzing the atmospheric processes that are conducive to the increase in O_3 concentration and the continuous exceedance of O_3 during TC activities, and found that the prevailing downdraft over the PRD brought meteorological conditions of clear sky, low wind speed, high boundary layer, and low relative humidity, which led to the continuous excess of O_3 concentration. Wang et al. (2024a) found that the continuous northward TCs produced and maintained meteorological conditions conducive to the generation of O_3, promoted the local accumulation and cross-regional transmission of O_3, and jointly led to a 30% increase in O_3 concentration in eastern China and a prolonged O_3 pollution period. Xu et al. (2023a) further revealed that when a typhoon landed in the YRD, the contribution of BVOC to O_3 in the Beijing-Tianjin-Hebei region reached 10 ppb; when the TCs moved to Beijing-Tianjin-Hebei region, the cross-transport between the northern China air mass and the YRD contributed half of the O_3 related to biological emissions. The peripheral winds and downdrafts of TCs lead to high temperatures and stable weather, which affect O_3 concentrations by affecting regional transport and biological emissions.

The Sixth Assessment Report of the Intergovernmental Panel on Climate Change (IPCC) pointed out that the rise in the average surface temperature of the earth caused by human activities has become a scientific consensus. Compared with the average surface temperature before industrialization (1850-1900), the global average surface temperature rose by about 0.8-1.3 ℃ due to human activities during 2010-2019 (Adak et al., 2023). In the context of global climate change, with the increases in greenhouse gas emissions, global warming, and interannual climate changes, the state of the atmosphere and ocean has changed, and sea-level rise and extreme climate events have occurred frequently, which have a low-frequency modulating effect on TCs. The activity characteristics of TCs have changed significantly, and rare high-intensity TCs have frequently made landfall in China (Wu, 2023). The southeastern coastal area, as one of the most economically developed and densely populated areas in China, is the area most seriously affected by TCs in China. Most TCs that affect China are generated in the northwest Pacific

https://doi.org/10.5194/egusphere-2025-2466
Preprint. Discussion started: 24 June 2025

Ocean, and their movement paths are affected by the WPSH. Before TCs make landfall from the northwest Pacific Ocean, China's coastal urban agglomerations often experience regional multi-day severe O_3 pollution (Wang et al., 2022b). Although the frequency of TCs in the northwest Pacific Ocean has decreased in recent years, their average intensity has shown an upward trend (Yu et al., 2025; Jung, 2025; Wang et al., 2022a) and their duration has also become longer (Nayak and Takemi, 2023). Yamaguchi and Maeda (2020) showed that although climate warming has accelerated the overall movement speed of TCs, their speed will slow down when they move toward the temperate zone during the poleward migration process, and the time they stay in a specific area will be extended. Affected by the surrounding atmospheric circulation, the slower the TCs move, the longer their impact time, and the greater the impact caused by the TCs, which will affect O_3 transmission, increase the duration of O_3 pollution, aggravate the degree of O_3 pollution, and expand the scope of pollution. In the context of global warming in the future, the increase in unfavorable meteorological conditions will make the O_3 pollution problem more serious (Fu and Tai, 2015; Keeble et al., 2017; Arnold et al., 2018; Akritidis et al., 2019; Saunier et al., 2020). Therefore, studying the trend of O_3 changes under future climate change scenarios is particularly important for formulating countermeasures against O_3 pollution.

The YRD is located in a key position in the eastern coastal economic zone of China. It is also a typical area frequently affected by TCs in the warm seasons (Wu et al., 2025; Qi et al., 2024). In addition, it has a high degree of urban agglomeration, dense population, and high energy consumption, making it a key prevention and control area for air pollution (Zhan et al., 2024; Bao et al., 2025). This study focuses on the regulatory mechanism of TCs on regional O_3 pollution and its impact on future pollution trends. First, based on the weather classification over the years, the characteristics of atmospheric circulation changes that cause O_3 changes are revealed, and the mechanism of TC weather pattern in the YRD affecting O_3 pollution is clarified. Secondly, based on the data reconstruction method, the O_3 annual variation series is reconstructed according to the frequency and intensity of SWPs. Finally, based on future scenario data, the evolution characteristics of atmospheric circulation and the trend in O_3 concentrations under different future scenarios are estimated, and the number of days when TC weather pattern appear and their contribution to O_3 variation are quantified. The research results help to fully and systematically understand the influence mechanism of weather conditions on O_3 pollution, provide a reference for the YRD to carry out targeted O_3 pollution control strategies, and have dual significance in improving regional air quality and advancing low-carbon development.

2 Materials and methods

2.1 O_3 observation data

The hourly pollutant monitoring data of 26 cities in the YRD used are derived from the National Environmental Monitoring Center of China. The platform provides pollutant concentration data updated every hour. To better describe the level of O_3 pollution at the urban scale, the arithmetic mean of the pollutant concentrations at each monitoring station was used as the pollutant concentration for the city. O_3-8h represents the daily 8h average O_3 concentration data, which can more accurately characterize the long-term exposure to regional O_3 pollution. Therefore, the O_3 data used in the analysis of this article all use the O_3-8h value, and the daily maximum 8-hour average concentration (unit: $\mu g/m^3$) is taken as the daily O_3 concentration.

https://doi.org/10.5194/egusphere-2025-2466
Preprint. Discussion started: 24 June 2025

2.2 Classification of synoptic weather patterns

Common objective weather classification methods mainly include principal component analysis, clustering algorithms, variance method based on correlation coefficient and neural network algorithm. We use orthogonal rotation principal component analysis in T mode (PTT) to classify SWPs in the YRD from 2018 to 2022. The PTT classification method has been integrated into the "cost733class" software. This method is an objective circulation classification method based on principal component analysis. By rotating the load of the T-mode principal component, its classification results are more physically interpretable (Philipp et al., 2016). It can accurately reflect the characteristics of the initial circulation field, does not change significantly due to different classification objects, and the obtained circulation spatio-temporal field is more stable (Huth et al., 2016). It has been widely used in research fields such as atmospheric circulation and air pollution (Hou et al., 2019; Gao et al., 2021).

The meteorological data are derived from the reanalysis data provided by the National Center for Environmental Prediction (NCEP). The dataset has a horizontal resolution of 2.5°×2.5°, with 144×73 grid points in the latitude-longitude domain and 17 vertical layers ranging from 1000 hPa to 10 hPa. Meteorological variables considered in this study include the 500 hPa geopotential height field, sea level pressure, 500 hPa wind field, 850 hPa wind field, 1000 hPa wind field, and vertical wind velocity. Considering that the 850 hPa geopotential height field effectively minimizes the influence of surface conditions on atmospheric motion while capturing the variations of shallow meteorological systems, this study utilizes the 850 hPa geopotential height field to classify SWPs and analyze the three-dimensional structure of circulation fields associated with different SWPs.

2.3 Reconstruction of annual variation series of O_3 concentration

The change in SWPs includes the changes in SWP frequency and intensity. The change in SWP frequency refers to the number of occurrences of a certain type of SWP in different years, while the change in SWP intensity refers to the change in the average intensity of the weather system associated with a certain type of SWP across different years. To quantify the contribution of the change in SWP frequency and intensity to the annual change of O_3, Yarnal (1993) proposed a method to assess the influence of changes in SWP frequency on the annual change of O_3. The specific equation is as follows:

$$\overline{\overline{O_{3m}}}(fre) = \sum_{k=1}^{6} \overline{O_{3k}}\, F_{km} \tag{1}$$

where $\overline{\overline{O_{3m}}}(fre)$ represents the reconstructed mean O_3 concentration influenced by the frequency variation in SWPs for year m; $\overline{O_{3k}}$ represents the average O_3 concentration of a certain SWP in all years, and F_{km} represents the frequency of occurrence of SWP for year m.

Later, Hegarty et al. (2007) proposed that the impact of SWP changes on the annual variation of O_3 should take into account changes in both frequency and intensity. Therefore, Eq. (1) was modified as follows:

$$\overline{\overline{O_{3m}}}(fre + int) = \sum_{k=1}^{6} (\overline{O_{3k}} + \Delta O_{3km}) F_{km} \tag{2}$$

where $\overline{\overline{O_{3m}}}(fre + int)$ represents the reconstructed mean O_3 concentration influenced by the frequency and intensity changes of SWPs for year m; ΔO_{3km} represents the modified anomaly concentration value obtained by fitting the SWP k intensity factor in the year m with the O_3 concentration anomaly value

https://doi.org/10.5194/egusphere-2025-2466
Preprint. Discussion started: 24 June 2025

(ΔO_3) for that year, which represents the oscillation of the O_3 concentration value caused by the change in the intensity of the SWP *k* in year *m*. Hegarty et al. (2007) used the average sea level pressure value in the classification area to represent the SWP intensity change factor. Liu et al. (2019) used the same method to construct the annual O_3 variation series in North China, but used the lowest pressure value in the classification area as the SWP intensity factor.

Since the characteristic changes of each SWP that lead to the increase in O_3 concentration are different, when defining the SWP intensity factor, it is necessary to consider the unique change characteristics that lead to the increase in O_3 concentration for each SWP. We define the SWP intensity factor in SWP1 as the maximum geopotential height in zone 1 (115°~135°E, 20°~40°N); SWP2 as the maximum geopotential height in zone 2 (90°~140°E, 20°~50°N); SWP3 and SWP5 as the minimum geopotential height in zone 3 (110°~130°E, 10°~40°N); and SWP4 as the average geopotential height in zone 2 (90°~140°E, 20°~50°N).

2.4 CMIP6 future climate scenario data

Based on 18 models of the Sixth International Coupled Model Intercomparison Project (CMIP6) and the ERA5 dataset, a bias-corrected global dataset was constructed (Xu et al., 2021). The dataset covers the historical period from 1979 to 2014 and the future climate scenarios from 2015 to 2100, with a horizontal grid spacing of 1.25°×1.25° and a time interval of 6 hours. Considering that O_3 pollution often occurs under extreme weather conditions, the more extreme SSP5-8.5 scenario was selected for this study. This scenario is a high-forcing scenario, and the radiative forcing stabilizes at 8.5 W/m^2 by 2100. In addition, as China implements more and more energy-saving and emission reduction measures, especially with the establishment of carbon peak and carbon neutrality goals, future greenhouse gas emissions are expected to be effectively controlled. Therefore, the relatively mild SSP2-4.5 scenario was selected for comparison. This scenario is a moderate forcing scenario, and the radiative forcing stabilizes at 4.5 W/m^2 by 2100. We use the 850 hPa average potential height field from 2018 to 2022 (historical period), 2030 (carbon peak), 2035 (beautiful China), 2060 (carbon neutrality), and 2100 to classify weather conditions.

3 Results and discussions

3.1 Characteristics of O_3 pollution in the YRD

Figure 1 shows the monthly trends of ground-level O_3 concentrations in the YRD from 2018 to 2022, inter-month variations of O_3 concentrations present a M-shaped pattern. From January to June, as the temperature rises and solar radiation increases, the O_3 concentration rises significantly and reaches the first peak (133.36 μg/m^3). However, the increased precipitation and higher humidity in July exert a notable wet scavenging effect on O_3 precursors. O_3 concentration increases again and reaches the second peak (126.38 μg/m^3) in September. From October to December, as the temperature gradually decreases and solar radiation weakens, the O_3 concentration shows a continuous downward trend, and reaches the lowest value of 54.17 μg/m^3 of the year in December. The O_3 concentration shows obvious seasonal changes throughout the year. In summer, higher temperatures, stronger solar radiation, and longer sunshine duration jointly enhance atmospheric photochemical reactions, thereby significantly increasing the O_3 concentration. In winter, lower temperatures, weaker solar radiation, and shorter sunshine duration lead to a significant weakening of photochemical reactions, which is not conducive to the generation of

https://doi.org/10.5194/egusphere-2025-2466
Preprint. Discussion started: 24 June 2025

O_3. From the kernel density curve, it can be seen that the distribution in summer months is wider, indicating that the O_3 concentration fluctuates greatly, while the distribution in winter months is narrower, indicating that the O_3 concentration changes are relatively stable in winter. This periodic variation reflects the high sensitivity of O_3 concentration in the YRD to meteorological conditions (temperature, solar radiation, humidity, wind speed, etc.), which affect the rate of photochemical reactions and thus affect the generation of O_3.

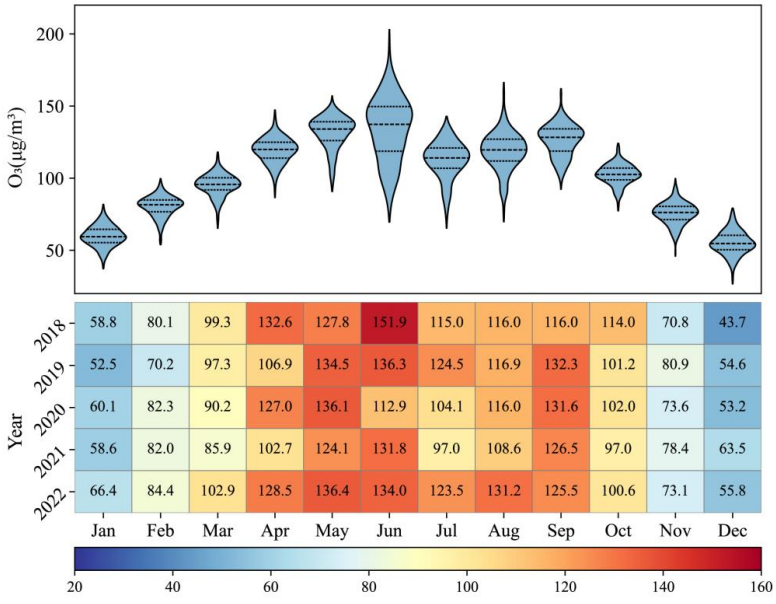

Figure 1. Inter-monthly variations of mean O_3 concentrations in the YRD from 2018 to 2021 (The region depicted in the violin plot corresponds to the kernel density curve, with the three black lines representing the 25th percentile, the mean, and the 75th percentile, respectively)

O_3 pollution in the YRD is concentrated in warm months of the year. We analyzed the temporal distribution of O_3 concentrations in representative cities in the YRD (Shanghai, Nanjing, Hangzhou, and Hefei) from April to September during 2018–2022 (Fig. 2). Since TCs mainly occur after June, and O_3 pollution is often associated with TC activity. During the same TC period, the O_3 concentrations in Shanghai, Nanjing, Hangzhou, and Hefei were different, but the temporal trends were similar. However, the spatiotemporal characteristics of O_3 pollution vary during different TCs and can be divided into two main trends: the O_3 concentration first increases and then decreases, or first increases, then decreases and then increases. The similarity is that when the TCs are generated, the O_3 concentrations in typical cities in the YRD are higher than the previous day. According to the evolution and trajectory of TC weather, TCs affecting China are primarily generated in the northwest Pacific Ocean. At this time, the YRD is located on the periphery of the TCs. Under the control of the periphery of the TCs, the strong downward airflow will make the YRD in stagnant weather conditions and inhibit the diffusion of pollutants (Shu et al., 2016), accompanied by high temperature, clear and dry weather conditions, which are the main weather conditions causing O_3 pollution. With the evolution of TC weather system, when the TCs center gradually approaches the YRD until it is within a certain range, the YRD is no longer under the influence

https://doi.org/10.5194/egusphere-2025-2466
Preprint. Discussion started: 24 June 2025

of the periphery of the TCs and comes under the control of the TC center, which is often accompanied by strong winds and precipitation, which significantly cleanse atmospheric pollutants, thereby reducing the O_3 concentration. Therefore, when the TCs gradually approach the YRD from the formation to the dissipation of the TCs, the YRD will change from being controlled by the periphery of the TCs to being controlled by the low-pressure center, thus forming a trend of O_3 concentration first increasing and then decreasing. After the TCs dissipate, O_3 levels may rise again due to restored meteorological conditions conducive to O_3 formation (Zhan et al., 2020). It can be seen that TCs may have an impact on the O_3 pollution in the YRD to a certain extent, highlighting the importance of implementing O_3 pollution control measures before TCs landfall.

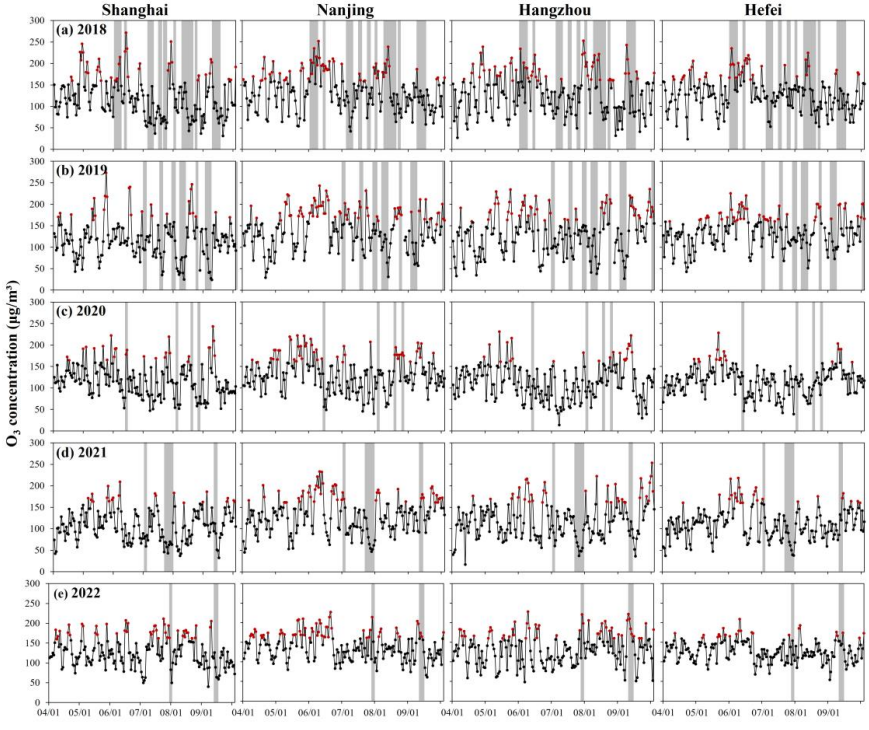

Figure 2. Changes in O_3 concentration in Shanghai, Nanjing, Hangzhou, and Hefei from April to September in 2018 to 2022. The gray shadows mark the time of impact of the TCs weather that landed, and the red dots are O_3-polluted days.

3.2 Main synoptic weather patterns in the YRD

To further explore the relationship between atmospheric circulation and O_3, the rotated orthogonal principal component analysis method was used to classify the weather in the YRD. The first dominant five SWPs were selected, and the remaining SWPs were defined as unclassified. A total of 1801 days were classified, and the remaining 25 days were unclassified weather patterns. As shown in Table 1, SWP1 and SWP2 are the main SWPs, with 980 and 570 days of occurrence, respectively, accounting for 53.67% and 31.22%. The occurrence frequencies of SWP3, SWP4, SWP5, and UP SWPs were lower, at 5.15%, 4.93%, 3.67%, and 1.37%, respectively. Table 1 also shows the seasonal occurrence frequencies

https://doi.org/10.5194/egusphere-2025-2466
Preprint. Discussion started: 24 June 2025

of the five SWPs, and the seasonal occurrence frequencies of each SWP differ significantly. SWP1 has the highest occurrence frequency in winter, at 44.39%, followed by spring (29.49%), autumn (24.80%), and summer (1.33%). SWP2 mainly occurs in summer, with the highest frequency in summer, reaching 66.49%, followed by spring (25.09%). SWP3 and SWP4 appear most frequently in autumn, at 79.79% and 68.89% respectively. SWP5 appears most frequently in summer (61.19%), followed by autumn (32.48%).

Statistics of O_3 concentration and meteorological factors under each SWP show that the average O_3 concentration for SWP1 is relatively low (87.60 μg/m^3), and the O_3 concentration under SWP2 reaches the highest (121.49 μg/m^3). The O_3 concentrations under SWP3, SWP4, and SWP5 are similar, which are 107.89 μg/m^3, 106.66 μg/m^3, and 109.50 μg/m^3 respectively. The difference in O_3 concentration under different SWPs is not only related to the seasonal frequency of occurrence but also closely related to the specific circulation field situation. For example, SWP2 and SWP5 with high O_3 concentrations are both SWPs with a higher frequency of occurrence in summer, but there are significant differences in O_3 concentrations between SWP2 and SWP5, which reflects the important influence of the circulation pattern on O_3 concentration. Specifically, SWP1 is mainly controlled by the northwest wind guided by the continental high pressure and the northeastern low pressure, SWP2 is mainly controlled by the southwest wind guided by the WPSH and the southwest vortex, SWP3 is mainly controlled by the southeast wind guided by the WPSH, SWP4 is mainly controlled by a saddle-shaped pressure field, mainly with northerly winds, and SWP5 is mainly controlled by the northeasterly winds influenced by the WPSH and TCs.

Table 1. The occurrence days and frequencies of various SWPs in the YRD from 2018 to 2022, the frequency of occurrence of each SWP across the four seasons, and the meteorological factors associated with each SWP.

Type	Number of days (frequency)	Seasonal occurrence frequency (%)				O_3 concentration (μg/m^3)	Temperature (℃)	Relative humidity (%)	Wind speed (m/s)
		Spring	Summer	Autumn	Winter				
SWP1	980(53.67%)	29.49	1.33	24.80	44.39	87.60	11.84	72.61	3.10
SWP2	570(31.22%)	25.09	66.49	6.32	2.11	121.49	25.58	77.39	3.23
SWP3	94(5.15%)	6.38	11.70	79.79	2.13	107.89	21.88	78.69	2.99
SWP4	90(4.93%)	15.56	13.33	68.89	2.22	106.66	21.79	75.93	2.94
SWP5	67(3.67%)	5.97	61.19	32.84	0.00	109.50	27.92	75.96	3.65
UP*	25(1.37%)	--	--	--	--	--	--	--	--

Notes: "*" Indicates weather conditions that were not classified and no statistical analysis was performed.

Figure 3 shows the three-dimensional atmospheric circulation structure of SWP1, SWP2, SWP3, and SWP4. For SWP1, the YRD is located east of the continental high pressure and southwest of the northeastern low pressure, and is affected by the northwest wind influenced by both the continental high pressure and the northeastern low pressure (at 850 hPa as shown in Fig. 3a). At sea level, the YRD is mainly controlled by the continental high pressure (Fig. 3e). At 500 hPa, the YRD is controlled by westerly winds (Fig. 3i). The adverse effects of low temperature and weak solar radiation in winter on O_3 photochemical reactions are the main reasons for the low O_3 concentration under SWP1.

For SWP2, the YRD is located to the northwest of the WPSH, and the southeast side is also affected by the southwest low vortex (Fig. 3j). At 850 hPa, the YRD is controlled by the southwest wind

https://doi.org/10.5194/egusphere-2025-2466
Preprint. Discussion started: 24 June 2025

influenced by the WPSH and the southwest vortex (Fig. 3b). The warmer southerly winds are conducive to the increase in temperature in the YRD, and high temperature is conducive to the photochemical reaction to produce O_3. At sea level, the WPSH shifts to the northeast, and the YRD is affected by the southerly wind (Fig. 3f). The southerly wind will transport pollutants from the PRD to the YRD. The combined effect of enhanced photochemical reactions and inter-regional advection transport causes the YRD to have a higher O_3 concentration under SWP2.

For SWP3, at 850 hPa, the YRD is located to the southwest of the WPSH and is controlled by the southeasterly winds at its southern edge (Fig. 3c). At sea level, the WPSH shifts northward, and the YRD is affected by northeasterly winds influenced by the tropical depression (Fig. 3g). At 500 hPa, the YRD is located at the edge of the WPSH or near the low-pressure trough (Fig. 3k). The intensity and position of the WPSH suppresses convective activity, resulting in the dominance of sinking airflow. Under SWP3, the YRD is controlled by southeasterly airflow from the ocean, which increases the regional humidity. As an autumn SWP, the average temperature of SWP3 is relatively low, and the meteorological conditions are generally not conducive to the generation of O_3 by photochemical reactions.

For SWP4, at 850 hPa, the YRD is mainly controlled by a saddle-shaped pressure field, located between two high-pressure systems and two low-pressure systems, and the wind speed in the YRD is relatively small (Fig. 3d). At sea level, the situation is similar (Fig. 3h). At 500 hPa, the YRD is located behind a weak trough (Fig. 3l), resulting in a weak subsidence near the surface. Under this weather situation, the YRD is mainly stagnant weather, and the subsidence and low horizontal wind speeds hinder the diffusion of pollutants, resulting in O_3 pollution.

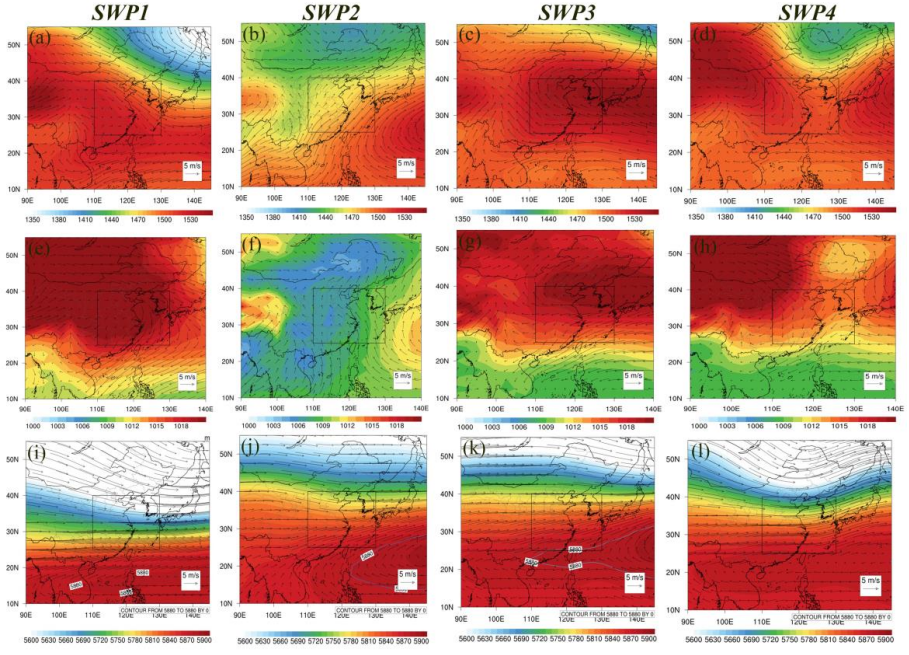

Figure 3. The average weather conditions in SWP1, SWP2, SWP3 and SWP4, including an 850 hPa geopotential height field superimposed on wind field **(a-d)**, sea level pressure field superimposed on 1000 hPa wind field **(e-h)**, a 500 hPa geopotential height field superimposed on wind field **(i-l)**. In **(a)-(l)**, shading represents geopotential height and black vectors represent wind. The black frame in **(a)-(i)** includes the YRD.

https://doi.org/10.5194/egusphere-2025-2466
Preprint. Discussion started: 24 June 2025

3.3 The important role of TCs on regional O_3 pollution

3.3.1 The impact of TC weather pattern (SWP5) on O_3 pollution in the YRD

Figure 4 shows the three-dimensional atmospheric circulation structure under the TC weather pattern (SWP5). For SWP5, similar circulation conditions are shown at 850 hPa (Fig. 4a) and sea level (Fig. 4b). The YRD is located to the northwest of TCs and is controlled by northeasterly winds guided by the TCs. The direction and intensity of the northeast wind have an important impact on the meteorological conditions and pollutant transport in the YRD. At 500 hPa, it is controlled by northerly or northwesterly flow (Fig. 4c). As SWP5 is a high-frequency pattern in summer, the meteorological factors of high temperature, low humidity, and strong solar radiation provide a favorable environment for photochemical reactions, thereby promoting the formation of O_3. At the same time, under the influence of lower-level TCs, the YRD is controlled by sinking airflow (Fig. 4d). The periphery downward airflows of the TCs make the atmosphere over YRD more stagnant, which cause the air hotter, dryer and more intense radiation (Table 1). This kind of weather pattern hinders the diffusion of pollutants, is easier for pollutants to accumulate in local areas, and thereby is conducive to the formation of O_3 accumulation.

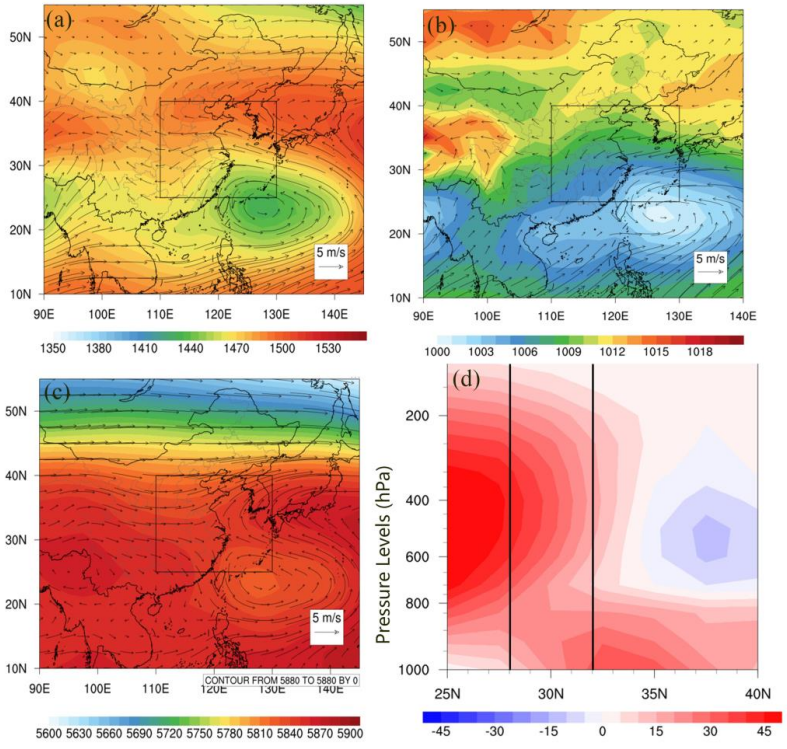

Figure 4. The average weather conditions in SWP5, including an 850 hPa geopotential height field superimposed on wind field **(a)**, sea level pressure field superimposed on 1000 hPa wind field **(b)**, a 500 hPa geopotential height field superimposed on wind field **(c)**, height-latitude cross-sections of vertical velocity (unit: 10^{-2} Pa·s^{-1}) between 25°N and 40°N **(d)**. In **(a)-(c)**, shading represents geopotential height and black vectors represent wind. The black frame in **(a)-(c)** and the vertical line area in **(d)** includes the YRD.

https://doi.org/10.5194/egusphere-2025-2466
Preprint. Discussion started: 24 June 2025

3.3.2 Changes of atmospheric circulation field with different O_3 pollution levels under TC weather pattern

To better explore the relationship between O_3 pollution and TC weather pattern (SWP5), O_3 pollution is further divided into clean type (C), local pollution type (LP), and regional pollution type (RP) according to the pollution characteristics. RP is defined as all days when more than 20% (> 5) of the 26 cities in the YRD have a maximum daily O_3 concentration of more than 160 μg/m^3, LP is defined as all days when fewer than 20% (< 5) of the 26 cities in the YRD have a maximum daily O_3 concentration of more than 160 μg/m^3, and C is defined as the remaining days excluding LP and RP. Table 2 shows the number of days and frequencies of C, LP, and RP under SWP5. Among them, the frequencies of SWP5_C, SWP5_LP, and SWP5_RP are 55.22%, 17.91%, and 26.87% respectively. The seasonal distribution characteristics of different degrees of O_3 pollution types in the TC weather pattern are further discussed. Under SWP5, the number of days of local pollution and regional pollution in the YRD is concentrated in summer and autumn. Local pollution is more likely to occur in autumn, with a frequency of 58.33%, and regional pollution is more likely to occur in summer, with a frequency of 72.22%.

Table 2. The number of days and frequency of occurrence of clean type (C), lightly polluted type (LP), and heavily polluted type (HP) under each SWP, the frequencies of their occurrence in four seasons.

Type		Number of days (and frequency in one SWP)	Seasonal occurrence frequency (%)			
			Spring	Summer	Autumn	Winter
SWP5	SWP5_C	37(55.22%)	10.81	62.16	27.03	0.00
	SWP5_LP	12(17.91%)	0.00	41.67	58.33	0.00
	SWP5_RP	18(26.87%)	0.00	72.22	27.78	0.00

Figure 5 shows the structural characteristics of the three-dimensional atmospheric circulation field with different O_3 pollution levels (SWP5_C, SWP5_LP, and SWP5_RP) under the SWP5. It illustrates that, for SWP5_C (Fig. 5a, d and g), the TCs are close to the YRD (Fig. 5d), and then bring strong winds and rainstorms to the YRD, which is not conducive to the accumulation of air pollutants and the generation of O_3 by photochemical reactions. At the same time, the high wind speed and rainfall scouring are conducive to the removal of pollutants. Therefore, clean days occur in the YRD under the influence of the TCs. For SWP5_LP (Fig. 5b, e and h), the TCs are located to the east of and a little far away from the YRD (Fig. 5). For the SWP5_RP (Fig. 5c, f and i), the center of TCs are located in the area around (25°N, 135°E). At 850 hPa (Fig. 5a, b and c), the changes of TCs are similar to those at 1000 hPa (Fig. 5d, e and f). At 500 hPa, a weak ridge appears as the pollution level deepens (Fig. 5g, h and i). The prevailing sinking airflow under the control of the WPSH can be strengthened by the TC activity, making the atmosphere more stagnant, and the meteorological conditions of high temperature and low humidity appear, causing the outbreak of O_3 pollution in the YRD (Shu et al., 2016). Among them, when local O_3 pollution occurs in the YRD, the TCs are slightly farther from the YRD, and their peripheral influence reaches the coastal areas (Fig. 5e). When regional O_3 pollution occurs in the YRD, the TCs are closer to the YRD, and their peripheral sinking effect is stronger over the YRD (Fig. 5f). In summary, when the TCs are located at 130°~135°E and 20°~30°N, the YRD is affected by the sinking airflow of the TCs, and high-concentration O_3 pollution is easily formed.

https://doi.org/10.5194/egusphere-2025-2466
Preprint. Discussion started: 24 June 2025

3.4 To what extent TCs impact regional O_3 pollution in the YRD

3.4.1 The role of changes in the intensity and frequency of SWPs in the reconstruction of the annual variation series of O_3

Figure 6 shows the annual variations of O_3 reconstruction concentrations from 2018 to 2022. It can be seen that when only the change in SWP frequency is considered, the reconstructed time series is relatively flat and cannot well show the downward trend of O_3 concentrations from 2019 to 2021. So, the change in SWP frequency has minimal impact on the annual variation of O_3. When the change in SWP intensity is considered, the reconstructed curve is closer to the original annual variation curve. Therefore, compared to the change in SWP frequency, the change in SWP intensity contributes more to the change in O_3 concentration. To accurately evaluate the impact of both SWP frequency and intensity on the annual variation of O_3 concentration, we quantitatively calculated the contribution of SWP frequency and intensity. The contribution index is defined as the ratio of the range (difference between the maximum and minimum values) of the reconstructed sequence to the range of the original sequence. When only the change in SWP frequency is considered, since the O_3 concentration value in 2020 is lower than that in 2021 in the reconstructed data, its reduction contribution rate is 0%, while when the change in SWP intensity is added, the reduction contribution rate is 81.39%. It can be seen that compared to the change in SWP frequency, the change in SWP intensity is a more significant factor contributing to the change in O_3 concentration.

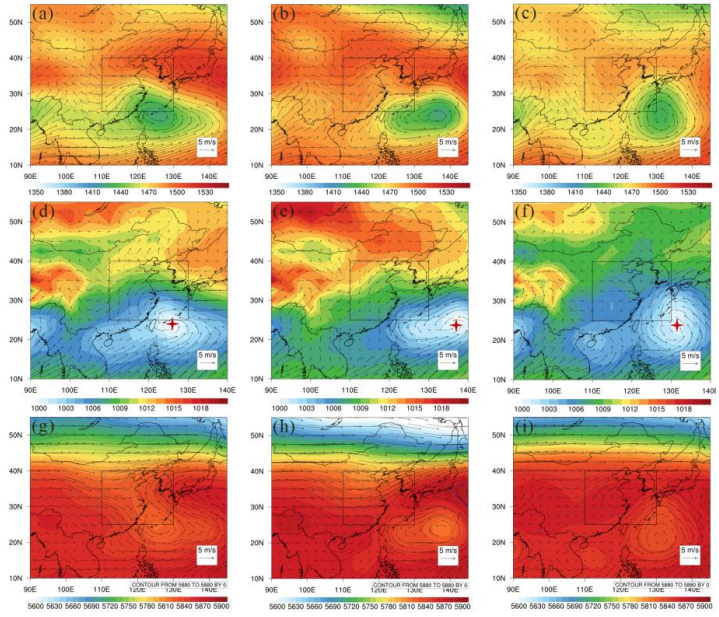

Figure 5. The average weather conditions in SWP5_C (left), SWP5_LP (middle), and SWP5_RP (right), including an 850 hPa geopotential height field superimposed on wind field **(a-c)**, sea level pressure field superimposed on 1000 hPa wind field **(d-f)**, a 500 hPa geopotential height field superimposed on wind field **(g-i)**. The shading represents geopotential height, black vectors represent wind and the black frame includes the YRD, and the red asterisk in **(d-f)** indicates the location where the TCs made landfall.

https://doi.org/10.5194/egusphere-2025-2466
Preprint. Discussion started: 24 June 2025

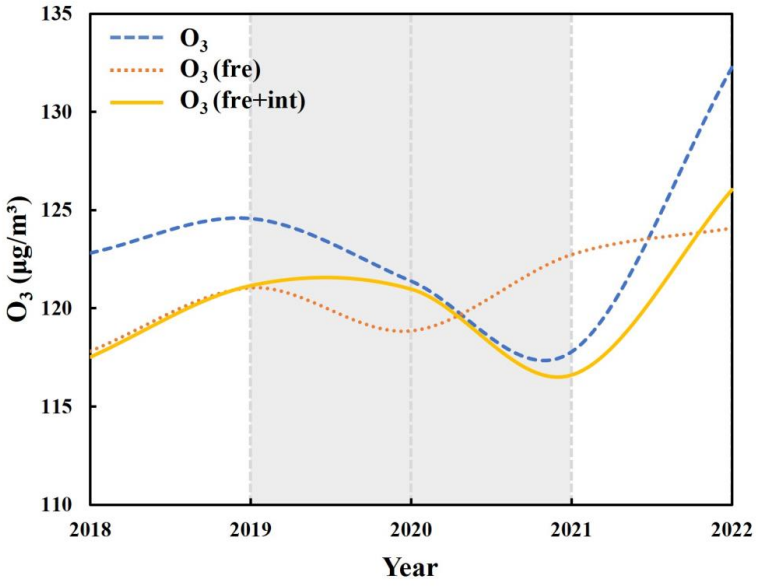

Figure 6. The interannual O_3 concentration trends for observed and reconstructed O_3 based on variations in SWPs in the YRD. The blue lines represent the observed interannual O_3 trend, whereas the orange and yellow lines are the trends of reconstructed O_3 concentrations according to the frequency-only and both frequency and intensity of SWP changes, respectively.

3.4.2 Changes in TCs and the effects on O_3 concentration over the YRD in the future

After clarifying the relationship between SWP and O_3 pollution, the trend of O_3 concentration change under different scenarios in the future can be estimated based on future SWP changes. O_3 pollution in the YRD mostly occurs during the warm seasons (April-September), so we analyzed the common SWP changes in the warm seasons of the YRD and the contribution of future SWP changes to the annual changes in O_3 concentration. Figure 7 shows the distribution of frequency of occurrence of each SWP in the warm seasons in the YRD under the historical period and the two future scenarios of SSP2-4.5 and SSP5-8.5. According to the average O_3 concentration of each SWP during the historical period, SWP1, SWP2, and SWP3 with higher O_3 concentrations are classified as high-average O_3 types. The average annual number of days in the historical period is 156.6. The high-average O_3 type has the highest frequency of occurrence in 2022 with higher O_3 concentrations (165 days). In the SSP2-4.5 future scenario, the high-average O_3 type appears 165, 179, 182, and 178 days in 2030, 2035, 2060, and 2100, respectively, showing an upward trend of varying degrees, with the largest number of days appearing in 2060. It can be inferred that if only SWP frequency changes are considered, O_3 concentration in 2060 will be higher under the SSP2-4.5 scenario. The high-average O_3 type appears 157, 161, 148, and 158 days in the SSP5-8.5 future scenario in 2030, 2035, 2060, and 2100, respectively. Except for 2060, the number of days with high O_3 concentration SWPs in the YRD increases slightly. Therefore, considering only SWP frequency changes, O_3 concentration in the YRD will increase under the SSP5-8.5 scenario, except in 2060.

https://doi.org/10.5194/egusphere-2025-2466
Preprint. Discussion started: 24 June 2025

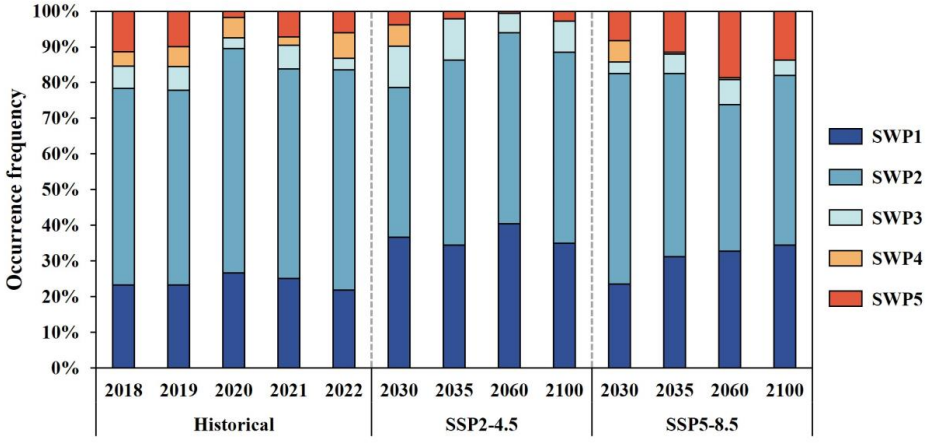

Figure 7. Frequency distribution of each SWP under the historical period, SSP2-4.5 and SSP5-8.5 future scenarios in the warm seasons over the YRD.

Due to the frequent occurrence of TCs during the warm seasons (Fig. 8), they not only bring extreme weather events but also have an important impact on regional O_3 pollution. We further studied the trend in the frequency of TC weather pattern. The SWP5 is influenced by TCs in the YRD. In the historical period (2018-2022), the average annual number of days when the TC weather pattern occurs in the YRD was 22.2 days. Under the SSP2-4.5 future scenario, there will be 28, 25, 11, and 21 days in 2030, 2035, 2060, and 2100 respectively. It can be seen that the number of days with TC weather pattern will increase to varying degrees in 2030 and 2035, while significantly decreasing in 2060. In the SSP5-8.5 future scenario, TC weather pattern will appear on 21, 31, 47, and 33 days in 2030, 2035, 2060, and 2100 respectively. Except for 2030, the number of days with SWPs controlled by TCs in the YRD will increase to varying degrees in future scenarios. Therefore, the frequency of TCs affecting O_3 concentration in the YRD is expected to increase significantly in the future under the SSP5-8.5 scenario.

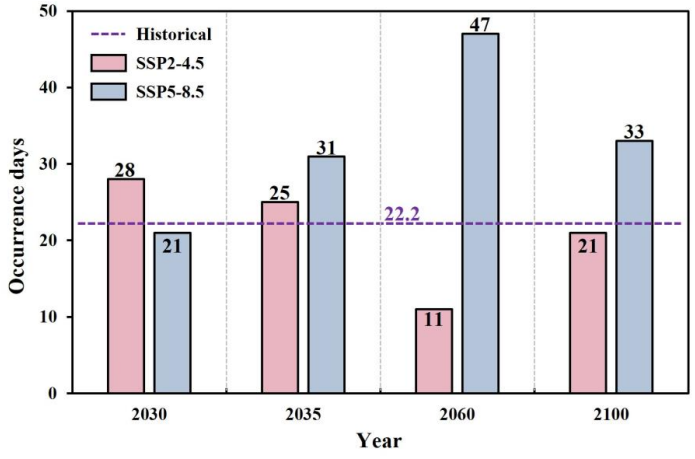

Figure 8. Occurrence days of TCs SWP under the historical period, SSP2-4.5 and SSP5-8.5 future scenarios in the warm seasons over the YRD.

https://doi.org/10.5194/egusphere-2025-2466
Preprint. Discussion started: 24 June 2025

3.4.3 Reconstruction of annual O_3 variability during warm seasons in the YRD under future scenarios

According to the weather classification results and the reconstructed empirical relationship, the O_3 concentration under the two future scenarios of SSP2-4.5 and SSP5-8.5 was estimated statistically. Figure 9 shows the predicted changes in future O_3 concentration and a comparison with the average O_3 concentration in the historical period. The average O_3 concentration in the warm seasons of the YRD from 2018 to 2022 is 123.76 μg/m^3. Under the SSP2-4.5 scenario, the future warm seasons O_3 concentration in the YRD will increase to varying degrees relative to the historical period, with an average increase of about 8.3 μg/m^3. Under the SSP5-8.5 scenario, the warm seasons O_3 concentration in the YRD will also increase to varying degrees compared with the historical period, with an average concentration increase of about 10.9 μg/m^3. In particular, the warm seasons O_3 concentration in the YRD will reach 146.72 μg/m^3 in 2100, which is about 23 μg/m^3 higher than the average warm seasons O_3 concentration in the historical period. In summary, under the two future climate scenarios of SSP2-4.5 and SSP5-8.5, the warm seasons O_3 concentration in the YRD shows an upward trend, with O_3 pollution more severe in the SSP5-8.5 scenario. The increase in high temperature, strong solar radiation, and calm weather caused by future climate warming is conducive to the generation and accumulation of O_3. The high intensity of precursor emissions in the SSP5-8.5 scenario further aggravates O_3 pollution.

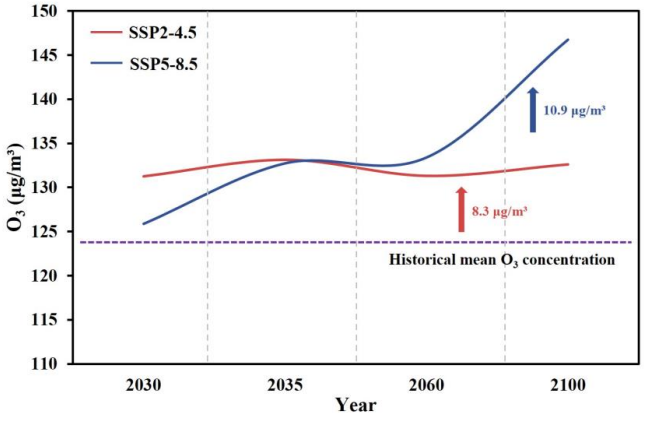

Figure 9. Estimation of O_3 concentration changes under SSP2-4.5 and SSP5-8.5 future scenarios based on intensity and frequency of SWPs, compared with the historical mean O_3 concentration.

We focus on the contribution of the TC weather pattern to the O_3 concentration under different future scenarios. Figure 10 shows the estimated contribution of each SWP to the future O_3 concentration. The SWP5 is influenced by TCs in the YRD. In the historical period (2018-2022), the average contribution of TCs to the warm seasons O_3 concentration in the YRD was 10.95%. Under the SSP2-4.5 scenario, the contribution of the TC weather pattern in 2030, 2035, 2060, and 2100 was 15.14, 9.97, 4.50, and 11.27%, respectively. Among them, the frequency of days controlled by the TC weather pattern in the YRD in 2060 was relatively low, resulting in a relatively low contribution of the TC weather pattern to the O_3 concentration in that year. Under the SSP5-8.5 scenario, the contribution of the TC weather pattern in 2030, 2035, 2060, and 2100 was 10.31, 14.50, 20.66 and 13.48%, respectively. It can be seen that under this scenario, except for 2030, the contribution of the TC weather pattern to O_3 pollution in the future

https://doi.org/10.5194/egusphere-2025-2466
Preprint. Discussion started: 24 June 2025

will increase to varying degrees compared with the historical period, that is, the TC weather pattern will have a significant impact on O_3 pollution in the YRD under this scenario.

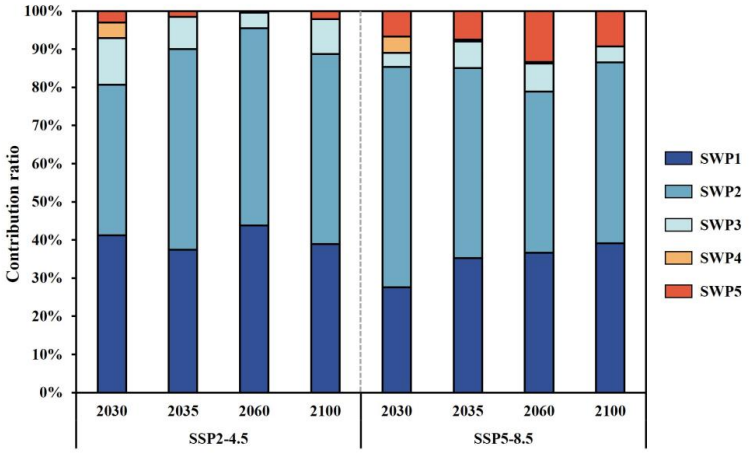

Figure 10. Contribution ratio of different SWPs to predicted O_3 concentrations under SSP2-4.5 and SSP5-8.5 future scenarios.

4 Conclusions

In response to the problem of O_3 pollution in the YRD, this paper studies the impact of weather conditions on O_3 pollution and future trends in the YRD, with special attention to the impact and mechanism of TCs on O_3 pollution. The spatial distribution characteristics of O_3 pollution and the changing characteristics during TC activity in the YRD from 2018 to 2022 were analyzed. The main SWPs in the YRD and their impact on varying levels of O_3 pollution were discussed using the PTT objective classification method. Finally, based on the reconstructed empirical relationship, the warm seasons O_3 concentration in the YRD under future scenarios was statistically estimated, and the contribution of TCs to future O_3 concentration changes. The main findings are as follows.

Analysis of O_3 pollution characteristics in the YRD from 2018 to 2022 shows that, affected by changes in temperature, solar radiation, and precipitation, inter-month variations of O_3 concentrations present an M-shaped pattern. Peaks generally occurring in June and September, and O_3 concentrations fluctuate greatly in summer. O_3 pollution in typical cities in the YRD during TC activity between 2018 and 2022 showed similar temporal variation trends, usually showing a pattern of first increasing and then decreasing, which is closely related to the path and center location of the TCs. When the TCs center is close to the YRD, the O_3 concentration in the region will decrease due to strong winds and rainfall, which is conducive to the removal of pollutants in the atmosphere. On the contrary, when the TCs are in the formation or dissipation stage, or their periphery airflows affecting the YRD, high temperature, sunny, and dry climate conditions are conducive to the formation and accumulation of O_3.

Through the PTT objective weather classification method, five dominant SWPs in the YRD were identified. SWP1 is mainly controlled by continental high and northeastern China low in the YRD, SWP2 is mainly controlled by the WPSH and southwest vortex, SWP3 is mainly controlled by the WPSH, SWP4 is mainly controlled by a saddle-pattern pressure field, and SWP5 is mainly controlled by the

https://doi.org/10.5194/egusphere-2025-2466
Preprint. Discussion started: 24 June 2025

WPSH and TCs. Among them, the high temperature in the region under SWP2 intensifies the photochemical reaction, and the south wind brings pollutants from the PRD, resulting in the highest O_3 concentration under SWP2. The average O_3 concentration under SWP5 is second high, mainly because the prevailing downdrafts controlled by the WPSH are strengthened due to TC activities, making the atmosphere more stagnant and affecting photochemical reactions and the transport and diffusion of pollutants.

The TC weather pattern (SWP5) is a high-frequency weather pattern in summer, with an occurrence frequency of 72.22%. The meteorological conditions of high temperature, low humidity, and strong solar radiation are conducive to the occurrence of photochemical reactions. For SWP5_LP and SWP5_RP, the prevailing downdrafts controlled by the WPSH will be strengthened by the TCs activities, making the air calm and stagnant, and the meteorological conditions of high temperature and low humidity will appear, causing the outbreak of O_3 pollution in the YRD. When the center of the TCs is located at 130°~135°E, 20°~30°N, the YRD is affected by the downdrafts outside the TCs, and high-concentration O_3 pollution is prone to form.

Based on data reconstruction, a statistical estimate of the warm seasons O_3 concentration in the YRD under future scenarios was made. Under the SSP2-4.5 scenario, it is estimated that the average O_3 concentration in the YRD in the future will be 8.3 μg/m^3 higher than in the historical period. Among them, the TC weather pattern contributes the most to the change in O_3 concentration in 2030, reaching 15.14%. Under the SSP5-8.5 scenario, the average concentration will increase by about 10.9 μg/m^3, especially by 2100, it is expected to be about 23 μg/m^3 higher than the current situation. In addition, the contribution of TC weather pattern to O_3 pollution is expected to increase under the SSP5-8.5 scenario, among which the contribution in 2060 will be the highest, reaching 20.66%. This indicates that under the scenario of intensified climate change, TC weather pattern will have a more significant impact on O_3 pollution in the YRD.

In summary, O_3 pollution in the YRD is on the rise, and summer O_3 pollution is often related to TC activities, and often occurs before and after TC activities. Through the research of this article, we have deepened our understanding of the mechanism of TCs on regional O_3 pollution. In addition, under the background of global warming, the intensity and duration of TC generation will increase, which will have a serious impact on China's coastal areas. Compared with the direct damage caused by landfalling TCs, the secondary disasters caused by them, such as O_3 pollution, should also be taken seriously. The research results have important scientific significance and practical application value for the in-depth understanding of the formation mechanism of O_3 pollution in the YRD, formulating targeted pollution prevention and control strategies, and improving regional air quality.

https://doi.org/10.5194/egusphere-2025-2466
Preprint. Discussion started: 24 June 2025

Data availability. Chinese O_3 monitoring data are available at http://www.cnemc.cn/en/. Meteorological data are available at http://rda.ucar.edu/datasets/ds083.2/. The TCs trajectory dataset are available at https://www.typhoon.org.cn/. CMIP6 future climate scenario data are available at https://www.scidb.cn/detail?dataSetId=791587189614968832.

Author contributions. MiX had the original ideas, MeX and YL collected and processed the data, designed the research and prepared the original draft. MiX discuss the results and revise the original draft and also provided financial support for the project leading to this publication. DM revised the paper and helped to collect the data. LF, SZ, SC and LH checked the English of the original paper.

Competing interests. The contact author has declared that none of the authors has any competing interests.

Financial support. This research has been supported by the National Nature Science Foundation of China (42275102), the Special Science and Technology Innovation Program for Carbon Peak and Carbon Neutralization of Jiangsu Province (BE2022612), the National Key Basic Research Development Program of China (2024YFC3711905) and the research start-up fund for the introduction of talents from Nanjing Normal University (184080H201B57).

https://doi.org/10.5194/egusphere-2025-2466
Preprint. Discussion started: 24 June 2025

References

Adak, S., Mandal, N., Mukhopadhyay, A., Maity, P. P., and Sen, S.: Current state and prediction of future global climate change and variability in terms of CO_2 levels and temperature, in: Enhancing resilience of dryland agriculture under changing climate: Interdisciplinary and convergence Approaches, Springer, 15-43, 10.1007/978-981-19-9159-2_2, 2023.

Akritidis, D., Pozzer, A., and Zanis, P.: On the impact of future climate change on tropopause folds and tropospheric ozone, Atmospheric Chemistry and Physics, 19, 14387-14401, 10.5194/acp-19-14387-2019, 2019.

Arnold, S. R., Lombardozzi, D., Lamarque, J. F., Richardson, T., Emmons, L. K., Tilmes, S., Sitch, S. A., Folberth, G., Hollaway, M. J., and Martin, M. V.: Simulated Global Climate Response to Tropospheric Ozone-Induced Changes in Plant Transpiration, Geophysical Research Letters, 45, 13070-13079, 10.1029/2018gl079938, 2018.

Bao, Q. Y., Lin, W. L., Jin, J. L., Xu, X. B., Zhao, G., Zhang, X. Y., and Ma, Q. L.: Long-term variation of O_3 in the Yangtze River Delta and its influencing factors from a regional perspective, Urban Climate, 60, 10.1016/j.uclim.2025.102353, 2025.

Chen, L., Zhu, J., Liao, H., Yang, Y., and Yue, X.: Meteorological influences on $PM_{2.5}$ and O_3 trends and associated health burden since China's clean air actions, Science of the Total Environment, 744, 10.1016/j.scitotenv.2020.140837, 2020.

Chow, E. C. H., Li, R. C. Y., and Zhou, W.: Influence of Tropical Cyclones on Hong Kong Air Quality, Advances in Atmospheric Sciences, 35, 1177-1188, 10.1007/s00376-018-7225-4, 2018.

Deng, T., Wang, T. J., Wang, S. Q., Zou, Y., Yin, C. Q., Li, F., Liu, L., Wang, N., Song, L., Wu, C., and Wu, D.: Impact of typhoon periphery on high ozone and high aerosol pollution in the Pearl River Delta region, Science of the Total Environment, 668, 617-630, 10.1016/j.scitotenv.2019.02.450, 2019.

Fu, Y. and Tai, A. P. K.: Impact of climate and land cover changes on tropospheric ozone air quality and public health in East Asia between 1980 and 2010, Atmospheric Chemistry and Physics, 15, 10093-10106, 10.5194/acp-15-10093-2015, 2015.

Gao, D., Xie, M., Liu, J., Wang, T. J., Ma, C. Q., Bai, H. K., Chen, X., Li, M. M., Zhuang, B. L., and Li, S.: Ozone variability induced by synoptic weather patterns in warm seasons of 2014-2018 over the Yangtze River Delta region, China, Atmospheric Chemistry and Physics, 21, 5847-5864, 10.5194/acp-21-5847-2021, 2021.

Gong, S. L., Zhang, L., Liu, C., Lu, S. H., Pan, W. J., and Zhang, Y. H.: Multi-scale analysis of the impacts of meteorology and emissions on $PM_{2.5}$ and O_3 trends at various regions in China from 2013 to 2020 2. Key weather elements and emissions, Science of the Total Environment, 824, 10.1016/j.scitotenv.2022.153847, 2022.

Gong, X., Sun, F. X., Wei, L., Zhang, Y., Xia, M. J., Ge, M., and Xiong, L. L.: Association of Ozone and Temperature with Ischemic Heart Disease Mortality Risk: Mediation and Interaction Analyses, Environmental Science & Technology, 58, 20378-20388, 10.1021/acs.est.4c05899, 2024.

Hegarty, J., Mao, H., and Talbot, R.: Synoptic controls on summertime surface ozone in the northeastern United States, Journal of Geophysical Research-Atmospheres, 112, 10.1029/2006jd008170, 2007.

Hou, X. W., Zhu, B., Kumar, K. R., and Lu, W.: Inter-annual variability in fine particulate matter pollution over China during 2013-2018: Role of meteorology, Atmospheric Environment, 214, 10.1016/j.atmosenv.2019.116842, 2019.

Hu, W. Z., Liu, R., Chen, Z. C., Ouyang, S. S., Hu, T. T., Wang, Y., Cui, Z. Y., Jiang, B., Chen, D. H., and Liu, S. C.: Processes conducive to high ozone formation in Pearl River Delta in the presence of

https://doi.org/10.5194/egusphere-2025-2466
Preprint. Discussion started: 24 June 2025

Pacific tropical cyclones, Atmospheric Environment, 307, 10.1016/j.atmosenv.2023.119859, 2023.

Huth, R., Beck, C., and Kucerová, M.: Synoptic-climatological evaluation of the classifications of atmospheric circulation patterns over Europe, International Journal of Climatology, 36, 2710-2726, 10.1002/joc.4546, 2016.

Jiang, Y. C., Zhao, T. L., Liu, J., Xu, X. D., Tan, C. H., Cheng, X. H., Bi, X. Y., Gan, J. B., You, J. F., and Zhao, S. Z.: Why does surface ozone peak before a typhoon landing in southeast China?, Atmospheric Chemistry and Physics, 15, 13331-13338, 10.5194/acp-15-13331-2015, 2015.

Jung, H.: Humans fuel stronger cyclones, Nature Climate Change, 15, 351-351, 10.1038/s41558-025-02321-1, 2025.

Keeble, J., Bednarz, E. M., Banerjee, A., Abraham, N. L., Harris, N. R. P., Maycock, A. C., and Pyle, J. A.: Diagnosing the radiative and chemical contributions to future changes in tropical column ozone with the UM-UKCA chemistry-climate model, Atmospheric Chemistry and Physics, 17, 13801-13818, 10.5194/acp-17-13801-2017, 2017.

Lam, K. S., Wang, T. J., Wu, C. L., and Li, Y. S.: Study on an ozone episode in hot season in Hong Kong and transboundary air pollution over Pearl River Delta region of China, Atmospheric Environment, 39, 1967-1977, 10.1016/j.atmosenv.2004.11.023, 2005.

Li, K., Jacob, D. J., Shen, L., Lu, X., De Smedt, I., and Liao, H.: Increases in surface ozone pollution in China from 2013 to 2019: anthropogenic and meteorological influences, Atmospheric Chemistry and Physics, 20, 11423-11433, 10.5194/acp-20-11423-2020, 2020.

Li, S., Gao, Y., Zhang, J., Hong, C., Zhang, S., Chen, D., Wild, O., Feng, Z., Xu, Y., and Guo, X.: Mitigating climate change and ozone pollution will improve Chinese food security, One Earth, 10.1016/j.oneear.2024.12.002, 2024.

Liu, J. D., Wang, L. L., Li, M. G., Liao, Z. H., Sun, Y., Song, T., Gao, W. K., Wang, Y. H., Li, Y., Ji, D. S., Hu, B., Kerminen, V. M., Wang, Y. S., and Kulmala, M.: Quantifying the impact of synoptic circulation patterns on ozone variability in northern China from April to October 2013-2017, Atmospheric Chemistry and Physics, 19, 14477-14492, 10.5194/acp-19-14477-2019, 2019.

Lu, H. X., Lyu, X. P., Cheng, H. R., Ling, Z. H., and Guo, H.: Overview on the spatial-temporal characteristics of the ozone formation regime in China, Environmental Science-Processes & Impacts, 21, 916-929, 10.1039/c9em00098d, 2019.

Nayak, S. and Takemi, T.: Statistical analysis of the characteristics of typhoons approaching Japan from 2006 to 2019, Geomatics Natural Hazards & Risk, 14, 10.1080/19475705.2023.2208722, 2023.

Philipp, A., Beck, C., Huth, R., and Jacobeit, J.: Development and comparison of circulation type classifications using the COST 733 dataset and software, International Journal of Climatology, 36, 2673-2691, 10.1002/joc.3920, 2016.

Qi, C. N., Wang, P. Y., Yang, Y., Li, H. M., Zhang, H., Ren, L. L., Jin, X. P., Zhan, C. C., Tang, J. P., and Liao, H.: Impacts of tropical cyclone-heat wave compound events on surface ozone in eastern China: comparison between the Yangtze River and Pearl River deltas, Atmospheric Chemistry and Physics, 24, 11775-11789, 10.5194/acp-24-11775-2024, 2024.

Saunier, A., Ormeño, E., Piga, D., Armengaud, A., Boissard, C., Lathière, J., Szopa, S., Genard-Zielinski, A. C., and Fernandez, C.: Isoprene contribution to ozone production under climate change conditions in the French Mediterranean area, Regional Environmental Change, 20, 10.1007/s10113-020-01697-4, 2020.

Shu, L., Xie, M., Wang, T. J., Gao, D., Chen, P. L., Han, Y., Li, S., Zhuang, B. L., and Li, M. M.: Integrated studies of a regional ozone pollution synthetically affected by subtropical high and typhoon system in

https://doi.org/10.5194/egusphere-2025-2466
Preprint. Discussion started: 24 June 2025

the Yangtze River Delta region, China, Atmospheric Chemistry and Physics, 16, 15801-15819, 10.5194/acp-16-15801-2016, 2016.

Wang, G. H., Wu, L. W., Mei, W., and Xie, S. P.: Ocean currents show global intensification of weak tropical cyclones, Nature, 611, 496-+, 10.1038/s41586-022-05326-4, 2022a.

Wang, J. H., Wang, P., Tian, C. F., Gao, M., Cheng, T. T., and Mei, W.: Consecutive Northward Super Typhoons Induced Extreme Ozone Pollution Events in Eastern China, Npj Climate and Atmospheric Science, 7, 10.1038/s41612-024-00786-z, 2024a.

Wang, N., Huang, X., Xu, J. W., Wang, T., Tan, Z. M., and Ding, A. J.: Typhoon-boosted biogenic emission aggravates cross-regional ozone pollution in China, Science Advances, 8, 10.1126/sciadv.abl6166, 2022b.

Wang, N., Wang, H. Y., Huang, X., Chen, X., Zou, Y., Deng, T., Li, T. Y., Lyu, X., and Yang, F. M.: Extreme weather exacerbates ozone pollution in the Pearl River Delta, China: role of natural processes, Atmospheric Chemistry and Physics, 24, 1559-1570, 10.5194/acp-24-1559-2024, 2024b.

Wang, Y., Yang, Y. J., Yuan, Q. Q., Li, T. W., Zhou, Y., Zong, L., Wang, M. Y., Xie, Z. Y., Ho, H. C., Gao, M., Tong, S. L., Lolli, S., and Zhang, L. P.: Substantially underestimated global health risks of current ozone pollution, Nature Communications, 16, 10.1038/s41467-024-55450-0, 2025.

Wang, Y. T., Zhao, Y., Liu, Y. M., Jiang, Y. Q., Zheng, B., Xing, J., Liu, Y., Wang, S., and Nielsen, C. P.: Sustained emission reductions have restrained the ozone pollution over China, Nature Geoscience, 16, 967-+, 10.1038/s41561-023-01284-2, 2023.

Wu, L. G., Yu, R. L., Xiang, C. Y., Yu, H., Feng, Y. C., and Zhou, X. Y.: Extreme Impacts of Four Landfalling Tropical Cyclones in China during the 2024 Peak Season, Advances in Atmospheric Sciences, 42, 817-824, 10.1007/s00376-025-4465-y, 2025.

Wu, S. H.: Research progress in climate change impact, risk, and adaptation: An interpretation of Part 2 of China's

Fourth National Assessment Report on Climate Change., China Population, Resources and Environment, 33, 80-86, 2023.

Xie, M., Zhu, K. G., Wang, T. J., Chen, P. L., Han, Y., Li, S., Zhuang, B. L., and Shu, L.: Temporal characterization and regional contribution to O_3 and NO_x at an urban and a suburban site in Nanjing, China, Science of the Total Environment, 551, 533-545, 10.1016/j.scitotenv.2016.02.047, 2016.

Xu, J. W., Zhou, D. R., Gao, J., Huang, X., Xue, L. K., Huo, J. T., Fu, Q. Y., and Ding, A. J.: Biogenic emissions-related ozone enhancement in two major city clusters during a typical typhoon process, Applied Geochemistry, 152, 10.1016/j.apgeochem.2023.105634, 2023a.

Xu, Y. F., Shen, A., Jin, Y. B., Liu, Y. M., Lu, X., Fan, S. J., Hong, Y. Y., and Fan, Q.: A quantitative assessment and process analysis of the contribution from meteorological conditions in an O3 pollution episode in Guangzhou, China, Atmospheric Environment, 303, 10.1016/j.atmosenv.2023.119757, 2023b.

Xu, Z. F., Han, Y., Tam, C. Y., Yang, Z. L., and Fu, C. B.: Bias-corrected CMIP6 global dataset for dynamical downscaling of the historical and future climate (1979-2100), Scientific Data, 8, 10.1038/s41597-021-01079-3, 2021.

Yamaguchi, M. and Maeda, S.: Slowdown of Typhoon Translation Speeds in Mid-latitudes in September Influenced by the Pacific Decadal Oscillation and Global Warming, Journal of the Meteorological Society of Japan, 98, 1321-1334, 10.2151/jmsj.2020-068, 2020.

Yang, J. X., Lau, A. K. H., Fung, J. C. H., Zhou, W., and Wenig, M.: An air pollution episode and its formation mechanism during the tropical cyclone Nuri's landfall in a coastal city of south China,

https://doi.org/10.5194/egusphere-2025-2466
Preprint. Discussion started: 24 June 2025

663 Atmospheric Environment, 54, 746-753, 10.1016/j.atmosenv.2011.12.023, 2012.
664 Yang, Z. Y., Li, Z. Q., Cheng, F., Lv, Q. C., Li, K., Zhang, T., Zhou, Y. Y., Zhao, B., Xue, W. H., and Wei,
665 J.: Two-decade surface ozone (O_3) pollution in China: Enhanced fine-scale estimations and
666 environmental health implications, Remote Sensing of Environment, 317, 10.1016/j.rse.2024.114459,
667 2025.
668 Yarnal, B.: Synoptic Climatology in Environmental Analysis A Primer, Journal of Preventive Medicine
669 Information, 347, 170-180, 10.1016/j.crte.2014.12.002, 1993.
670 Yu, X. C., Lei, Y. D., Wang, Z. L., Zhao, D. J., Li, Y. F., Liu, L., Wu, B., Che, H. Z., and Zhang, X. Y.:
671 Inhomogeneous aerosol forcing increasing tropical cyclone intensity in western North Pacific by
672 weakening vertical wind shear, Environmental Research Letters, 20, 10.1088/1748-9326/adb766,
673 2025.
674 Zhan, C. C. and Xie, M.: Land use and anthropogenic heat modulate ozone by meteorology: a perspective
675 from the Yangtze River Delta region, Atmospheric Chemistry and Physics, 22, 1351-1371,
676 10.5194/acp-22-1351-2022, 2022.
677 Zhan, C. C., Xie, M., Huang, C. W., Liu, J. N., Wang, T. J., Xu, M., Ma, C. Q., Yu, J. W., Jiao, Y. M., Li,
678 M. M., Li, S., Zhuang, B. L., Zhao, M., and Nie, D. Y.: Ozone affected by a succession of four landfall
679 typhoons in the Yangtze River Delta, China: major processes and health impacts, Atmospheric
680 Chemistry and Physics, 20, 13781-13799, 10.5194/acp-20-13781-2020, 2020.
681 Zhan, Y. Z. H., Xie, M., Zhuang, B. L., Gao, D., Zhu, K. G., Lu, H., Wang, T. J., Li, S., Li, M. M., Luo,
682 Y., and Zhao, R. Q.: Particle-ozone complex pollution under diverse synoptic weather patterns in the
683 Yangtze River Delta region: Synergistic relationships and the effects of meteorology and chemical
684 compositions, Science of the Total Environment, 946, 10.1016/j.scitotenv.2024.174365, 2024.
685 Zhang, Z. K., Lu, B. Q., Liu, C., Meng, X., Jiang, J. K., Herrmann, H., Chen, J. M., and Li, X.: Nitrate
686 pollution deterioration in winter driven by surface ozone increase, Npj Climate and Atmospheric
687 Science, 7, 10.1038/s41612-024-00667-5, 2024.
688 Zhao, S. P., Yin, D. Y., Yu, Y., Kang, S. C., Qin, D. H., and Dong, L. X.: $PM_{2.5}$ and O_3 pollution during
689 2015-2019 over 367 Chinese cities: Spatiotemporal variations, meteorological and topographical
690 impacts, Environmental Pollution, 264, 10.1016/j.envpol.2020.114694, 2020.
691